Supercond. Sci. Technol. **11** (1998) 13–20. Printed in the UK PII: S0953-2048(98)88136-0

Microstructure of $YBa_2Cu_3O_{7-\delta}$ Josephson junctions in relation to their properties

K Verbist†, O I Lebedev†¶, M A J Verhoeven‡, R Winchern‡, A J H M Rijnders‡, D H A Blank‡, F Tafuri§, H Bender‖ and G Van Tendeloo†

† EMAT, University of Antwerp (RUCA), Groenenborgerlaan 171, B-2020 Antwerp, Belgium
‡ Department of Applied Physics, University of Twente, POB 217, 7500 AE Enschede, The Netherlands
§ Dipt. Scienze Fisiche, University of Naples 'Federico II', P. le Tecchio 80, 80125 Naples, Italy
‖ IMEC, Kapelstraat 75, B-3001 Leuven, Belgium

Received 1 July 1997

Abstract. The microstructure of various types of Josephson junctions is investigated with cross-sectional (CS) high-resolution electron microscopy (HREM). Special specimen preparation techniques, to facilitate the CS investigation, are discussed in the first part. Examples are shown of specially produced arrays of junctions and of the focused ion beam thinning technique allowing us to investigate specific measured junctions. Ramp-type junctions with $PrBa_2Cu_{3-x}Ga_xO_{7-\delta}$ (PrBCGaO) barrier layers are discussed in more detail in the second part. The microstructure of PrBCGaO ($0.1 < x < 1.0$) thin films, barrier layers and bulk material is studied by HREM. Thin barrier layers with $x \geq 0.7$ contain a Ga-rich intergrowth, never observed before in YBCO-type structures. Ga-rich inclusions in single thin films exhibit a similar structure. In addition, diffusion of Ga in the ion-etched $SrTiO_3$ substrate surface region was observed. The observed segregation of Ga from the PrBCGaO barrier layer explains the observed junction properties.

1. Introduction

Josephson junctions (JJs) based on the high-T_c superconductor $REBa_2Cu_3O_{7-\delta}$ (REBCO), with RE = rare earth, can be fabricated by sandwiching a thin barrier of non-superconducting material between two superconducting electrodes. Alternatively, a grain boundary grown in a controlled way, a so-called artificial grain boundary (AGB), can also exhibit JJ properties. A microstructural characterization is of great importance for the measured properties to be correctly interpreted. Cross-sectional (CS) high-resolution electron microscopy (HREM) offers the possibility to obtain local structural information from the junction area itself in addition to the characterization of the film and interface quality. The fabrication of JJs is a highly technological process in which various processing steps can influence the obtained results. This should be taken into account to interpret the measured electrophysical properties.

To be able to reach the principal aim of this HREM study, to establish a correlation between microstructure and measured physical properties of JJs, it is necessary to identify fabrication influences and EM sample preparation artefacts. The CS sample preparation of JJs for HREM investigations is 'the' determining factor for a successful study but is unfortunately not trivial. Two different approaches are discussed in this study. The first approach is the use of an array of junctions (multiple junctions) to enhance the chance of finding a junction along the row with suitable thickness to allow HREM imaging. The other approach is to use the focused ion beam (FIB) thinning technique to allow the investigation of a very specific region, i.e. the 'barrier' of a measured junction.

Secondly a specific problem for which a correlation between measured properties and microstructure could be established is discussed in detail. The microstructure of $PrBa_2Cu_{3-x}Ga_xO_{7-\delta}$ as a function of the Ga substitution level is investigated. Thin $PrBa_2Cu_{3-x}Ga_xO_{7-\delta}$ ($x \geq 0.7$) barrier layers in ramp-type JJs and thin films of $PrBa_2Cu_{3-x}Ga_xO_{7-\delta}$ ($x = 0.1, 0.4, 0.7$) are characterized by HREM. The substitution of Ga in PrBCGaO bulk material and its structure are verified from XRD and HREM.

¶ On leave from Institute of Crystallography, Leninsky pr. 59, 117333 Moscow, Russia.

0953-2048/98/010013+08$19.50 © 1998 IOP Publishing Ltd

These studies are performed by scanning electron microscopy (SEM), selective area electron diffraction (SAED), transmission electron microscopy (TEM), high-resolution electron microscopy (HREM) and energy-dispersive X-ray spectroscopy (EDS).

2. Experimental details

The preparation of the trilayers with PrBCO and selective epitaxially grown (SEG) patterned films is reported in [1]. Further references to the SEG process can be found in [2]. The preparation of the bi-epitaxial artificial grain boundary junctions is reported in [3]. The patterning of the 10 μm wide junctions was done by standard photolithographic means with a dilute HNO_3 etching. The preparation of the ramp-type JJs is briefly as follows [4, 5]. The E1 base electrode (DyBCO) and the separating (S) insulating layer (PrBCO) have been deposited *in situ*. The ramps are structured by an Ar ion beam source (under an angle of 45°) using a photoresist mask. After stripping the photoresist, the ramp surface is cleaned by ion-milling and re-oxygenized *in situ*. Subsequently, the B barrier layer (PrBCGaO) and the top electrode (E2) (DyBCO) are deposited. The Ga content of barrier layer is nominal. A schematic drawing with the naming scheme is shown as part of figure 4.

CS samples for TEM are mechanically polished with a tripod on diamond lapping foils followed by ion thinning. High-resolution (HREM) and electron diffraction (ED) investigations are performed with a JEOL 4000 EX and a Philips CM 20 microscope equipped with a Link EDS detector. All CS EM micrographs of *c*-axis multilayers shown here are recorded with the [001] axis of the REBCO layers perpendicular to the electron beam.

CS TEM specimens from patterned and measured JJs are prepared by an FIB [6]. The patterned microbridge (width 2–10 μm) selected for FIB preparation is cut from the sample as a small strip and first polished in such a way that the area of interest is lying in the middle of a sliver of 20–30 μm thickness. This specimen is glued on a large-slot copper grid and mounted in the FIB instrument. As almost no contrast difference is present between the YBCO structure and the surrounding substrate on the FIB image, first some marks are put on the specimen by milling some craters with the FIB. The exact location of the JJ is then optically measured with respect to these marks and these coordinates are used for further thinning of the specimen. This is done by stepwise milling from the top of the specimen with decreasing ion beam currents to a depth of approximately 4 μm, so that finally a thin slice of about 15 μm width and less than 50 nm thickness remains at the selected area. A protective Pt layer is deposited *in situ* in the FIB instrument in order to protect the surface during the intermediate imaging to follow the progress of the milling procedure.

3. Results and discussion

3.1. Viewing junctions in CS HREM

The multiple-junction approach can easily be used for junction fabrication processes using masks. Usually the mask is replaced by a mask consisting of a multiple of the original mask. For instance, ramp-type JJs made by ion etching of a single-line photoresist mask can be fabricated by ion etching a multiple-line mask. The structure of multiple junctions can vary despite the fact that all involved parameters, except the mask, are kept constant. It is important to recognize the variations that are due to the multiple-mask preparation. Two examples are discussed here.

The ramp-type junctions studied here are made on purpose with a multiple mask (spacing 10 μm masked, 10 μm unmasked) using the same deposition procedures as for the operational junctions, i.e. ion beam etching to create the ramp slope. It was clearly noted that there is an inhomogeneous distribution of the ion-beam flux resulting in a difference of the amount of material removed over the 1 cm $\times$ 1 cm substrate. It can happen that 20 nm of $SrTiO_3$ is etched away at the foot of a certain edge while 20 nm of base electrode still remains near the foot of another edge, at a distance of nearly 1.4 cm on the substrate from the first edge. As a result the etching procedure can be incomplete, i.e. some of the DyBCO not covered by photoresist remains on the substrate. Incomplete etching enhances the possibility of undesired direct connections between the electrodes. This problem is specific to the multiple mask used for the EM study with 1000 edges cm^{-1}; for electrical measurements only five junctions are created on a substrate.

The second example is planar *a*-axis junctions patterned by the SEG procedure. *a*-axis trilayers are not easily patterned and the SEG technique represents a valid alternative. The predeposited titanium layer is already patterned and the overgrowing *a*-axis YBCO 'respects' this pattern since on titanium a polycrystalline film is formed with a lot of secondary phase inclusions and the YBCO is non-superconducting owing to the Ti pollution. The investigated substrate was patterned with 20 μm Ti lines and a YBCO/PrBCO/YBCO *a*-axis oriented trilayer was grown on a PrBCO template covering the complete substrate. From the SEM image the very rough film on the Ti layer can easily be distinguished form the film on $SrTiO_3$ (figure 1(*a*)). The EM observations clearly demonstrated the *c*-axis nature of the multilayer, especially in the vicinity of the Ti layer (figure 1(*b*)). Further away from the latter, a mixed *a*-and *c*-axis growth was noticed. The identical deposition procedure was repeated for an untreated substrate and clearly *a*-axis growth was observed for all the layers except the PrBCO template near the $SrTiO_3$ interface (figure 1(*c*)). This illustrates that the multiple mask technique in this case modified the heat behaviour of the substrate considerably, leading to a modified growth of the film.

The ultimate goal of correlating measured properties and microstructure on the same junction can be obtained by using the FIB technique. This technique allows us to

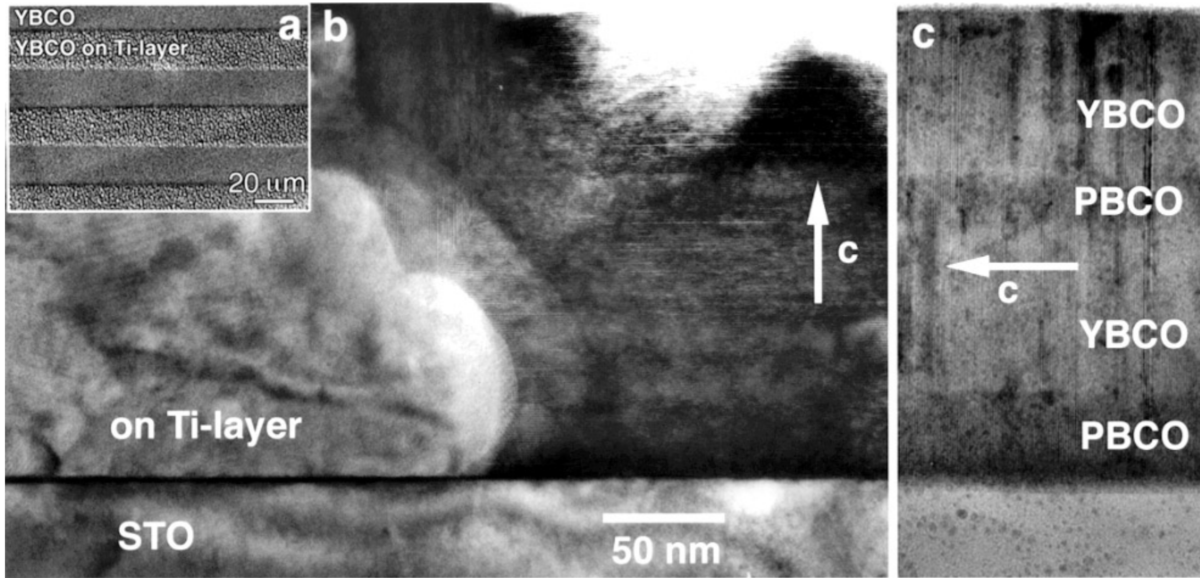

Figure 1. (*a*) SEM image showing the YBCO film grown on titanium with a very rough surface and the YBCO film grown on the bare $SrTiO_3$ substrate. The line spacing is 20 μm. (*b*) CS image showing the *c*-axis orientation of the YBCO/PrBCO/YBCO/PrBCO multilayer near the Ti layer. (c) CS image showing the *a*-axis orientation of the YBCO/PrBCO/YBCO/PrBCO multilayer grown under identical conditions on a substrate without Ti lines.

prepare a CS specimen at a very specific site (micrometre range) with a higher success rate than conventional CS preparation techniques based on Ar ion beam milling. This technique, which uses a Ga ion source, is well established for semiconductor devices. The FIB equipment allows us, in combination with CS TEM preparation to deposit metal contact paths, to cut contact paths and to obtain images based on secondary electron emission.

Various patterned and measured bi-epitaxial JJs are prepared by an FIB as CS samples. These junctions consist of 45° *a* (or *b*) tilt or twist boundaries obtained by growing (103)–(013) YBCO on (110) $SrTiO_3$ and (001) YBCO on MgO buffered (110) $SrTiO_3$. The results shown here are for 10 μm thick junctions across a 45° *a* (or *b*) twist boundary. The transport measurements are summarized as follows. The magnetic and temperature dependence of the critical current gave evidence of its Josephson nature. The magnetic modulation was more than 50%. Despite the fact that the pattern exhibited the maximum at zero voltage, deviations from the ideal Fraunhofer pattern were also observed. The shape of I–V curves was typical of the RSJ model, with the presence of an excess current and of resonance steps at voltages of the order of 300 μV. These steps are usually referred to as Fiske steps (we verified their dependence on the magnetic field) and from their position it is possible to estimate the ratio between the thickness barrier and the dielectric constant (in this case 0.03 nm). The critical current density J_c is 1.3×10^4 A cm^{-2} at $T = 4.2$ K, while the specific conductance is of the order of 100 $(\mu\Omega\ \mathrm{cm}^2)^{-1}$. The maximum working temperature of the junction was 75 K. The I_cR_n value with R_n the normal resistance, a quality factor of junctions for various applications, is 1 meV at $T = 4.2$ K. Figure 2(*a*) shows an optical micrograph on which the measured junction is arrowed. Figure 2(*b*) shows the 10 μm wide microbridge. Figure 2(*c*) shows the CS TEM image. The end of the MgO buffer layer is indicated. Some etching has occurred in the neighbouring $SrTiO_3$. The interface between (001) YBCO and (103)–(013) YBCO is mostly along the [001] direction of the (001) film. No secondary phase is present at the interface.

3.2. Ramp-type JJs with PrBCGaO barrier layers

The product of the critical current and the normal state resistance is an important figure of merit for JJs. The use of $PrBa_2Cu_{3-x}Ga_xO_{7-\delta}$ (PrBCGaO) as a barrier layer produces junctions with a higher normal state resistance than unsubstituted PrBCO while it leaves the critical current unaffected [4].

Cu can be substituted by Ga in ceramic PrBCO for substitution levels in the range $0.01 < x < 0.9$ [7]. Thin films produced from $PrBa_2Cu_{3-x}Ga_xO_{7-\delta}$ single targets have been grown by various methods [4, 8, 9]. The resistivities of the thin films are systematically lower and are increasing at a lower rate than those of the bulk samples [4]. No clear reason for this difference was proposed. To our knowledge there are no reports of structural differences between PrBCGaO bulk materials and thin films. *A priori* no indications exist that allow us to assume a difference between PrBCGaO bulk materials and thin films. However, in the light of our findings obtained from thin films we characterized the bulk material that was used as target to allow a comparison.

XRD shows that the $PrBa_2Cu_{3-x}Ga_xO_{7-\delta}$ samples have a structure identical to that of tetragonal $ReBa_2Cu_3O_{7-\delta}$. No Ga-containing impurity phase is present in PrBCGaO with $x = 0.7$ indicating the full substitution of Cu by Ga. The unit cell parameters are $a = 0.392\,88(6)$ nm and $c = 1.1756(5)$ nm. These are in good agreement with the

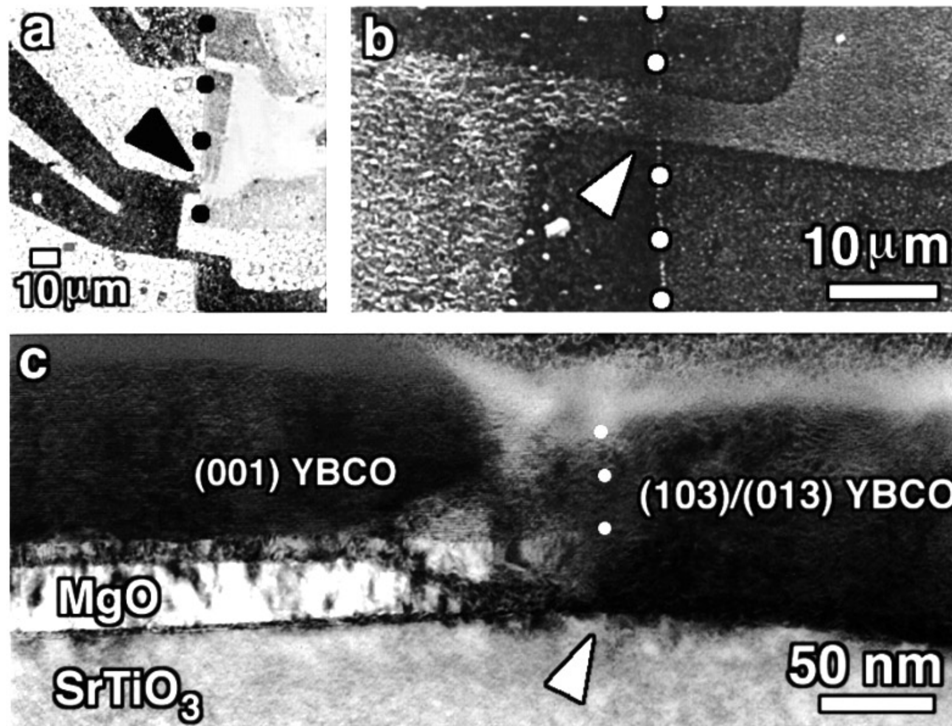

Figure 2. (*a*) Optical micrograph with the measured junction arrowed. (*b*) SEM image showing the bi-epitaxial grain boundary (arrowed) and the junction bridge patterned across it. Notice the difference in roughness between (001) YBCO and (103)–(013) YBCO films. (*c*) Cross-sectional TEM overview of the grain boundary. The end of the MgO buffer layer is indicated. The interface between the (001) and (103)/(013) YBCO films is mostly along the [001] direction of the (001) film.

values reported by [7]. For the substitution level $x = 1$ two impurity phases were found, namely CuO and α-$BaGa_2O_4$. The fact that a Ga-containing phase is present as an impurity phase indicates that $x = 1$ is above the maximum substitution level for Ga in $PrBa_2Cu_{3-x}Ga_xO_{7-\delta}$. Bulk $PrBa_2Cu_{3-x}Ga_xO_{7-\delta}$ with $x \geq 0.7$ has been investigated by EM and SAED. The reciprocal space contains no extra spots or streaks and no spot splitting. There is no modulation or structural change of the REBCO structure, detectable by HREM, due to the Ga substitution in the Cu(1) chain.

Electrical measurements of ramp-type JJs with PrBCGaO barriers ($x = 0.1$ and 0.4) have been reported previously [4, 10]. Briefly, the effect of a PrBCO barrier layer with Ga substitution on the junction parameters is an increase in the resistivity up to an order of magnitude for the same barrier thickness as compared with junctions with unsubstituted PrBCO as a barrier. However, this trend is not continued for the higher substitution levels $x = 0.7$ and 1. On the contrary, no increase in resistivity for $x = 0.7$ was observed as compared with $x = 0$ (figure 3).

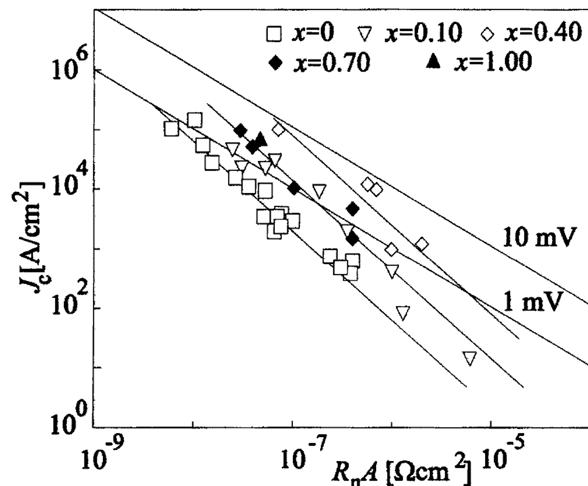

Figure 3. The critical current density J_c versus the R_nA product (R_n being the normal resistance and A the area of the junction) for ramp-type junctions with $PrBa_2Cu_{3-x}Ga_xO_{7-\delta}$ barriers having x = 0, 0.1, 0.4, 0.7, 1.0. No increase in resistivity for x = 0.7 and 1.0 compared with x = 0.4 was observed.

A CS EM investigation provides information about the local structure of the barrier layer as incorporated in the JJ. We concentrate ourselves here on the special features in the PrBCGaO barrier layer. Other aspects of the microstructure of these JJs have been reported in [11, 12]. No special features were found at the interfaces or inside the superconducting layers responsible for the abnormal behaviour of JJs with substitution levels $x = 0.7$ or 1 for the barrier layer. The junctions discussed here have a ramp angle of 21° and a barrier layer thickness of 10–30 nm (figure 4). All layers grow epitaxially with c-axis orientation perpendicular to the substrate. All interfaces in the unetched part and etched part are sharp and flat. The interfaces between barrier and superconducting layers at the ramp edge are well defined and free of secondary phases or

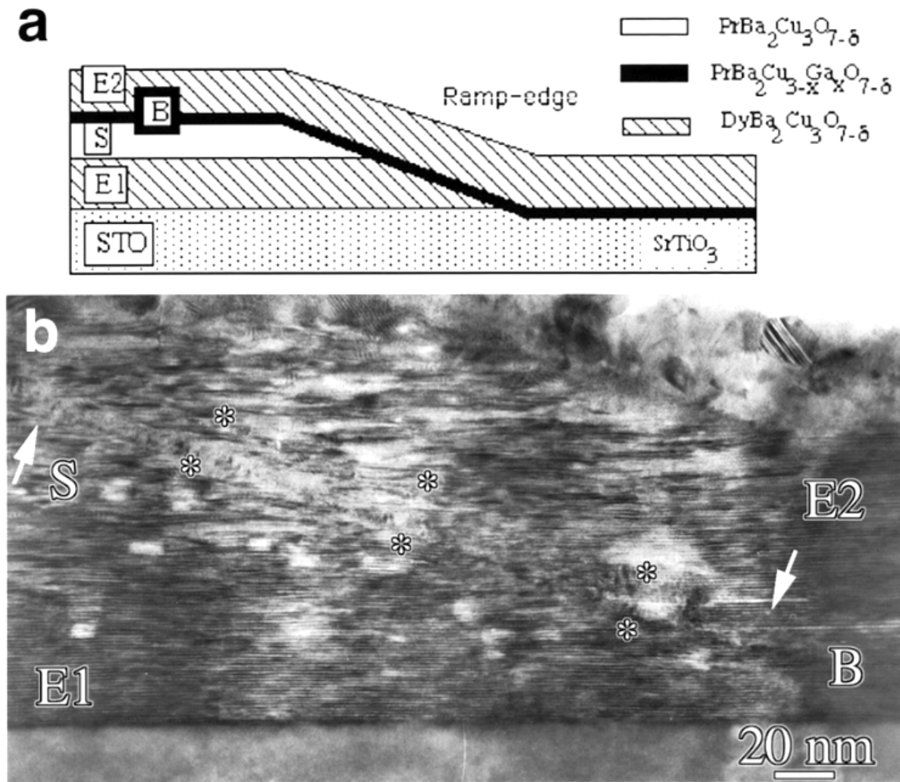

Figure 4. (*a*) Schematic representation of the investigated ramp-type junctions. (*b*) HREM overview of a ramp-type JJ with a PrBCGaO barrier of 10 nm, showing that the interfaces at the ramp are well defined and free of secondary or amorphous phases.

amorphous layers (figure 4(*b*)). This allows us to correlate the observed microstructure of the $PrBa_2Cu_{3-x}Ga_xO_{7-\delta}$ barrier layer and the electrical properties of the ramp-type JJs with this barrier material.

The HREM image of figure 5(*a*) shows part of a 30 nm thick PrBCGaO barrier layer ($x = 0.7$) grown on the ion-etched substrate. The barrier layer contains isolated unit cells with *c*-axis lengths different from c_{123}, indicated by double arrows on figure 5. These defective stacking sequences can have lengths along a up to 10 nm and are found throughout the complete barrier layer thickness. These unit cells with spacings in the c direction of approximately $c_i = 0.8$ nm differ from the normal 123 structure and are not known as common defects in 123. They are perfectly intergrown in the 123 environment and tend to grow as a periodic intergrowth within the 123 structure. The intergrowth occurs only in the $PrBa_2Cu_{2.3}Ga_{0.7}O_{7-\delta}$ barrier layer, not in the DyBCO bottom or top layer or in the PrBCO separating layer. If the Ga content is increased to 33% ($PrBa_2Cu_2Ga_1O_{7-\delta}$) the frequency of the c_i unit cell is increased. The presence of Ga seems to favour the presence of the intergrowth.

Taking into account all these data we propose a model for the Ga-containing intergrowth layer which has an a parameter very close to that of PrBCO and which fits epitaxially to PrBCO in the *a*–*b*-plane. Figure 5(*c*) shows an image averaged along the a direction. The CuO planes are indicated by single white arrows. There is a clear inequivalence in contrast between the CuO planes (I) and the plane in the middle of the intergrowth unit cell (II). The contrasts above and below the CuO planes are similar. The contrast strongly resembles that of a double perovskite with an inequivalent lattice plane in the middle of the cell. Together with the frequency of the intergrowth cell in the stacking (i.e. of the middle plane) as a function of the substitution level, this was interpreted as the occurrence of a full Ga plane and Ga-based compounds with this feature were evaluated. The compound $PrSrGaCuO_5$ was described by Roth *et al* [13]. The lattice parameters are $a = 1.633\,58$ nm, $b = 0.550\,02$ nm and $c = 0.535\,34$ nm with space group $Ima2$. The tetrahedral oxygen coordination of Ga induces a shift of the Ga and O positions from the ideal perovskite positions. This feature is important in view of the inequivalent contrast between planes I and II. A model based on one slab of $PrSrCuGaO_5$ sandwiched between PrBCO unit cells was created for image simulations. Sr was replaced by Ba in the model. The layer stacking is PrBCO–CuO–(Pr,Ba)O–GaO–(Pr,Ba)O–CuO–PrBCO. Ga and its surrounding oxygens are shifted from the ideal perovskite positions owing to the tetrahedral coordination of Ga. The image simulations based on this model yield a good agreement with the observed HREM image.

Pronounced black patches are observed in the $SrTiO_3$ substrate in the uppermost 10 nm of the interface region with the barrier layer in the two-layer part; such defects are indicated by arrows in figure 6(*a*). No dislocation can be observed, however. This specific contrast exists in all parts of the $SrTiO_3$ substrate, even on the inclined

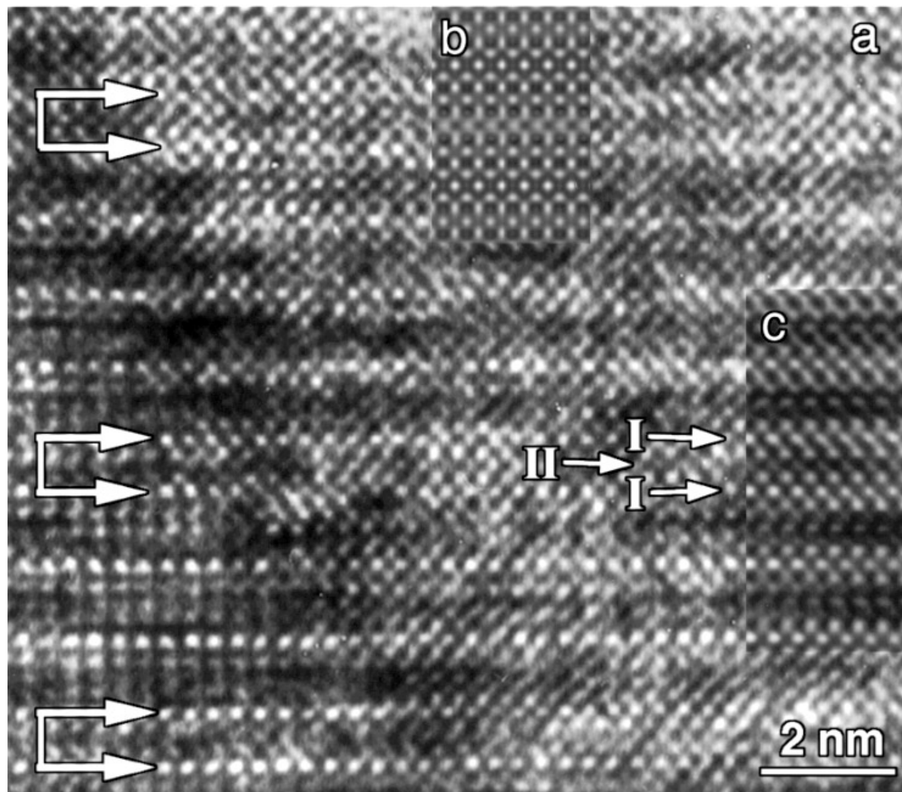

Figure 5. (*a*) [001] HREM micrograph of the intergrowth with c_i unit cell in the 123 structure observed in a PrBCGaO barrier layer ($x = 0.7$). Notice the perfect intergrowth along *a* and *c* directions. (*b*) Simulated image for $d = 2.4$ nm; $\delta = -25$ nm based on the proposed model. (*c*) Part of the image averaged along the *a* direction showing clearly the inequivalent contrast in the planes I (CuO planes of PrBCGaO structure) and plane II.

ramp edge in $SrTiO_3$, which has been exposed to Ar etching to create the ramp edges. Such contrast variations are normally not observed for ReBCO films on $SrTiO_3$ and were not observed in the neighbouring four-layer part of the junction. This rules out ion-beam thinning for EM specimen preparation as a possible origin. Possible other causes could be oxygen depletion or interdiffusion either of the photoresist material or of gallium from the barrier layer. Figure 6(*b*) shows a [100] HREM image of the interface between $PrBa_2Cu_{2.3}Ga_{0.7}O_{7-\delta}$ and pristine $SrTiO_3$. No black patches can be observed in the substrate. Figure 6(*c*) shows the interface of a $DyBa_2Cu_3O_{7-\delta}$ layer on an ion-etched $SrTiO_3$ substrate. It is clearly observed that the particular contrast of black patches only exists in figure 6(*a*) and is absent in figures 6(*b*) and 6(*c*). This proves that the contrast of black patches is only observed for the combination of a Ga-containing layer on an ion-etched $SrTiO_3$ substrate. Only ion etching is insufficient to produce this contrast. Therefore we believe that Ga diffusion in the surface region of the ion-etched $SrTiO_3$ substrate is the reason for the local structural distortions. This can be understood if we assume that lattice imperfections, such as oxygen vacancies or point defects which are created in the $SrTiO_3$ substrate by the ion etching, facilitate the diffusion of gallium in the interface region of the substrate.

We conclude that two distinct mechanisms of Ga segregation in thin barrier layers are operative; the formation of a Ga-containing intergrowth in the barrier layer itself and diffusion of Ga in the ion-etched substrate. The microstructure of $PrBa_2Cu_{3-x}Ga_xO_{7-\delta}$ ($x = 0.7$ or 1) thin barrier layers is clearly different from the one in bulk material.

The microstructure of PrBCGaO barriers with $x = 0.1$ or 0.4 was investigated from thin films of 20 and 80 nm thickness deposited on $SrTiO_3$ substrates under identical conditions to those during the JJ fabrication. No intergrowth with a *c*-spacing of 0.8 nm or secondary phase inclusions could be observed inside the films. A high density of defects of the types 124 and 224 was observed and results in a highly distorted crystal lattice. Occasionally an outgrowth of the Ga phase was observed at the surface of the thicker films. More outgrowths and inclusions inside the film are observed as the Ga nominal substitution level increases and the same trend holds for a given *x* value as the film thickness increases. A clear example of an inclusion observed in a 100 nm thick film of $PrBa_2Cu_{3-x}Ga_xO_{7-\delta}$ with $x = 0.7$ is shown in figure 7. The composition was found to be Ga rich as compared with the surrounding 123. The Ga phase has lattice parameters 0.8 nm, 0.41 nm and $\alpha \approx 92°$. The Ga-rich phase exhibits, as a separate inclusion, no fixed orientation relation with the surrounding 123. The contrast resembles that of the intergrowth and fits well the simulations of the $PrSrCuGaO_5$ structure. Probably by replacing Sr by Ba a monoclinic distortion is introduced

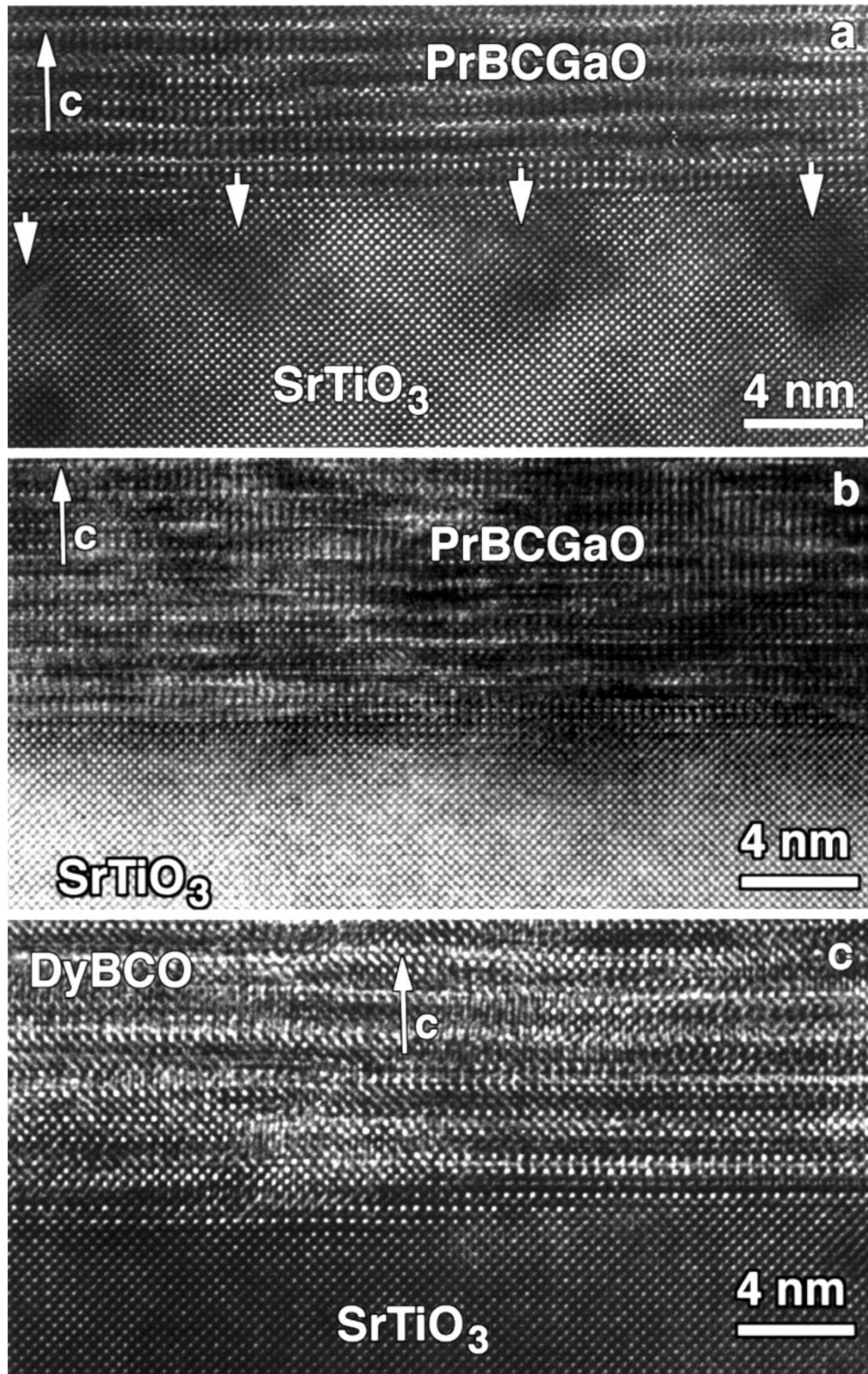

Figure 6. [001] HREM micrographs of the interface between (*a*) $PrBa_2Cu_{2.3}Ga_{0.7}O_{7-\delta}$ and ion-etched $SrTiO_3$ (dark contrast areas in the substrate are indicated by arrows), (*b*) $PrBa_2Cu_{2.3}Ga_{0.7}O_{7-\delta}$ and bare $SrTiO_3$ and (*c*) $DyBa_2Cu_3O_{7-\delta}$ and ion-etched $SrTiO_3$. In the latter two cases the dark contrast areas are absent.

in the structure owing to the larger size of the cation. We believe that this phase is related to the intergrowth described above although the intergrowth is rarely observed in the thin films of PrBCGaO. The growth conditions for a thin barrier layer on a substrate allowing Ga diffusion with a top layer preventing surface segregation differ clearly from the growth on a pristine substrate with an uncovered surface. We believe that the intergrowth is stabilized under 'barrier layer' growth conditions but grows as separate inclusions in thin films of $PrBa_2Cu_{3-x}Ga_xO_{7-\delta}$ with high x. We would

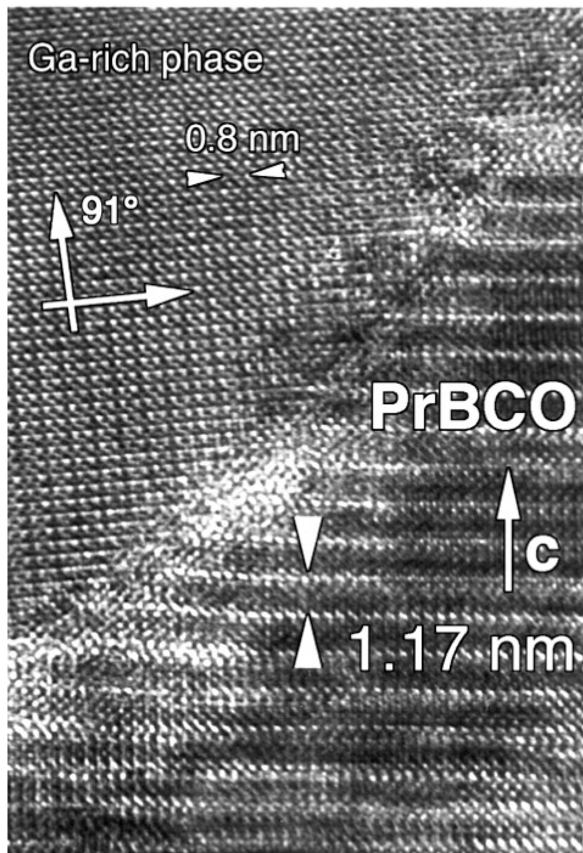

Figure 7. Ga-rich inclusions in a 100 nm thick film of $PrBa_2Cu_{2.3}Ga_{0.7}O_{7-\delta}$.

like to stress that the size of the Ga-rich inclusions is too small (50–200 nm) to be detected by XRD and these films show only 00*l* peaks of the 123 structure in XRD plots.

4. Conclusion

The CS sample preparation is an important aspect for a successful study of the microstructure of JJs. Influences on the microstructure from fabrication procedures and TEM sample preparation can be recognized. The FIB preparation technique allows us to characterize by HREM the junction area of a measured JJ. This was demonstrated for a bi-epitaxially grown 45° *a* (or *b*) axis twist grain boundary junction.

The behaviour of the junction parameters of REBCO ramp-type JJs with $PrBa_2Cu_{3-x}Ga_xO_{7-\delta}$ barrier layers at high Ga substitution levels is better understood thanks to a TEM microstructural characterization. Deviations from the structure of $PrBa_2Cu_{3-x}Ga_xO_{7-\delta}$ as the bulk ceramic powder were observed in barrier layers and thin films. A Ga-rich intergrowth was detected in the barrier layers together with the diffusion of Ga in the ion-etched substrate. Thin single films of $PrBa_2Cu_{3-x}Ga_xO_{7-\delta}$ with $x \geq 0.7$ contain Ga-rich inclusions but intergrowths are rarely observed. $PrBa_2Cu_{3-x}Ga_xO_{7-\delta}$ with $x = 0.1$ and 0.4 can be used as a barrier layer in ramp-type JJs to enhance reproducibly the normal state resistivity although higher Ga substitutions are not effective.

Acknowledgments

The authors wish to thank L Rossou and G Stoffelen for the excellent EM sample preparation. This research is part of the EC project on Novel Superconductors no CHRX-CT94-0461. This text presents partial research results of the Belgian IUAP programme. The scientific responsibility is assumed by the authors.

References

[1] Winchern R G 1997 Planar high-T_c Josephson junctions *PhD Thesis* University of Twente
[2] Damen C A J, Kropman B L, Blank D H A and Rogalla H 1995 *Applied Superconductivity 1995 (Inst. Phys. Conf. Ser. 148)* ed D Dew-Hughes (Bristol: Institute of Physics) p 859
[3] Di Chiara A, Lombardi F, Milletto Granozio F, Scotti di Uccio U, Tafuri F and Valentino M 1997 *IEEE Trans. Appl. Supercond.* **7** 3327
[4] Verhoeven M A J, Gerritsma G J, Rogalla H and Golubov A A 1995 *IEEE Trans. Appl. Supercond.* **5** 2095
[5] Verhoeven M A J, Gerritsma G J and Rogalla H 1995 *Applied Superconductivity 1995 (Inst. Phys. Conf. Ser. 148)* ed D Dew-Hughes (Bristol: Institute of Physics) p 1395
[6] Young R J, Kirk E C, Williams D A and Ahmed H 1990 *Mater. Res. Soc. Symp. Proc.* **199** 205
[7] Xu Y and Guan W 1993 *Physica* C **206** 59
[8] Sodtke E, Andrzejak C, Guggi D and Xu Y 1991 *Physica* C **180** 50
[9] Contour J P, Sant C, Ravelosona D, Fisher B and Patlagan L 1993 *Japan. J. Appl. Phys.* **22** L1143
[10] Verhoeven M A J, Gerritsma G J, Rogalla H and Golubov A A 1996 *Appl. Phys. Lett.* **69** 849
[11] Verbist K, Lebedev O I, Van Tendeloo G, Verhoeven M A J, Rijnders A J H M and Blank D H A 1996 *Proc. Eur. Conf. on Electron Microscopy XI, EUREM '96 (UCD Bellfield, Dublin)*
[12] Verbist K, Lebedev O I, Van Tendeloo G, Verhoeven M A J, Rijnders A J H M and Blank D H A 1996 *Supercond. Sci. Technol.* **9** 978
[13] Roth G, Adelmann P, Knitter R, Massing S and Wolf T 1992 *J. Solid State Chem.* **99** 376